

Journal of Materials Chemistry B

Accepted Manuscript



This is an *Accepted Manuscript*, which has been through the Royal Society of Chemistry peer review process and has been accepted for publication.

Accepted Manuscripts are published online shortly after acceptance, before technical editing, formatting and proof reading. Using this free service, authors can make their results available to the community, in citable form, before we publish the edited article. We will replace this *Accepted Manuscript* with the edited and formatted *Advance Article* as soon as it is available.

You can find more information about *Accepted Manuscripts* in the [Information for Authors](#).

Please note that technical editing may introduce minor changes to the text and/or graphics, which may alter content. The journal's standard [Terms & Conditions](#) and the [Ethical guidelines](#) still apply. In no event shall the Royal Society of Chemistry be held responsible for any errors or omissions in this *Accepted Manuscript* or any consequences arising from the use of any information it contains.

Multifunctional self-assembled cationic peptide nanostructures efficiently carry plasmid DNA in vitro and exhibit antimicrobial activity with minimal toxicity

Santosh Yadav^{a,†}, Manohar Mahato^a, Rajiv Pathak^b, Diksha Jha^b, Bipul Kumar^b, Smriti Rekha Dekha^a, Hemant Kumar Gautam^b and Ashwani Kumar Sharma^{a,*}

^aNucleic Acids Research Laboratory, CSIR-Institute of Genomics and Integrative Biology, Mall Road, Delhi – 110007, India

^bMicrobial Biotechnology Laboratory, CSIR-Institute of Genomics and Integrative Biology, Sukhdev Vihar, Mathura Road, Delhi – 110020, India

[†]Academy of Scientific and Innovative Research, New Delhi, India

Address for correspondence

Dr. Ashwani Kumar Sharma
Nucleic Acids Research Laboratory,
CSIR-Institute of Genomics and Integrative Biology,
Mall Road, Delhi – 110007, India
Email: ashwani@igib.res.in
Tel.: +91 11 27662491
Fax: +91 11 27667471

Abstract

In this study, a modified dehydropeptide, Boc-F Δ F- ϵ Ahx-OH, was conjugated with an aminoglycoside antibiotic, Neomycin, to construct a multifunctional conjugate, Pep-Neo. The amphiphilic conjugate (Pep-Neo) was able to self-assemble into cationic nanostructures in an aqueous solution at low concentrations. The nanostructure formation was evidenced via TEM and dynamic light scattering analyses. The average hydrodynamic diameter of self-assembled Pep-Neo nanostructures was found to \sim 279 nm with zeta potential of +28 mV. The formation of nanostructures with hydrophobic core and cationic hydrophilic shell resulted in an increased local concentration of cationic charge (*ca.* in 50% aqueous methanol, i.e. disassembled structure, zeta potential decreased to +17.6 mV), leading to efficient interactions with negatively charged plasmid DNA (pDNA). The size and zeta potential of the resulting Pep-Neo/pDNA complex were found to be \sim 154 nm and +19.4 mV, respectively. Having been characterized by physicochemical techniques, the complex was evaluated for the toxicity and ability to deliver nucleic acid therapeutics. Flow cytometry results on MCF-7 cells revealed that Pep-Neo/pDNA complex transfected \sim 27% cells at w/w ratio of 66.6 while the standard transfection reagent, Lipofectamine, could transfect only \sim 15% cells. MTT and hemolysis assays showed the non-toxic nature of the projected conjugate at various concentrations. Further, these nanostructures were shown to encapsulate hydrophobic drugs in the core. Finally, Pep-Neo nanostructures showed efficient antibacterial activity against different strains of gram positive and gram negative bacteria. Interestingly, unlike neomycin (which is highly effective against gram negative bacteria), these nanostructures showed considerably high efficiency against gram positive strains ensuring promising potential of these nanostructures for various biomedical applications.

Introduction

With the due advancement in the field of gene therapy, nonviral vectors have attracted the attention of researchers and shown their potential to carry nucleic acids to their targets inside the cells.^{1,2} However, a safe and efficient delivery system with multifunctional activity, inherent biodegradability and biocompatibility is still elusive. Recently, synthetic cationic peptide-based vectors have been extensively studied for this purpose due to their superior properties,³⁻⁸ however, suboptimal ability to protect themselves as well as bound nucleic acids under cellular environment limit their widespread use in biomedical sciences.

Of late, self-assembly of amphiphilic peptides has emerged as novel nanomaterials in the area of nanobiotechnology.⁹⁻¹³ These materials have been shown to withstand high temperature conditions, extreme pH range, many digesting enzymes and denaturants. Bearing good biocompatibility with cultured mammalian cells, these do not elicit immune response when introduced into animals. These properties have made them ideal candidates for tissue engineering

and drug delivery. Recently, these carriers have been used for the delivery of nucleic acids, drugs, peptides, proteins and small molecules of pharmaceutical importance.⁵⁻¹⁵ Amphiphilic peptide-based carriers bearing unique properties self-assemble to generate nanostructures mimicking viral vectors but having higher gene/drug loading capability. In continuation to our recent work focused on development of efficient vectors for gene delivery,¹⁴ here, in the present investigation, we have designed and synthesized a novel multifunctional conjugate via coupling of a modified small dehydropeptide, Boc-Phe-dehydro-Phe- ϵ -aminohexanoic acid (Boc-F Δ F- ϵ Ahx-OH), with an aminoglycoside antibiotic, Neomycin, that self-assembles to generate nanostructures having hydrophobic core and hydrophilic shell structure. Neomycin is a natural aminoglycoside with a branched structure having aminosugars joined by glycosidic bonds. Most of the aminoglycosides possess natural affinity for double stranded DNA, however, neomycin has shown least affinity towards these molecules.¹⁵ Recently, aminoglycoside-based hyperbranched polymers have been shown to exhibit good transfection efficiency, antitumor and antibacterial activities.¹⁶⁻¹⁸ Here, while designing the projected amphiphilic conjugate, it was anticipated that neomycin would not only introduce cationic charge density to the conjugate but also make it water soluble to work under physiological conditions. The projected conjugate would also bear multifunctional properties in terms of biological activity, stability under cellular environment and ability to encapsulate drugs in the hydrophobic core and transfer genetic material inside the cells. Hence, by conjugating a branched hydrophilic structure (Neomycin) with hydrophobic dipeptide, the resulting amphiphilic Pep-Neo conjugate would self-assemble into nanostructures with hydrophilic cationic charged moieties on the surface, which would interact with the negative charged nucleic acids and facilitate their entry into the cells. Following this strategy, an amphiphilic Pep-Neo conjugate was synthesized and after physicochemical characterization, it was evaluated for its transfection efficacy and cytotoxicity on mammalian cells. Further, two hydrophobic molecules (eosin and curcumin) were entrapped in the hydrophobic core of these nanostructures. Elucidating the multifunctional character of the conjugate nanostructures, its antibacterial activity was examined on various gram-positive and gram-negative strains. Apart from biodegradable and biocompatible, enhanced transfection efficiency with negligible toxicity of these nanostructures along with ability to encapsulate drug molecules confirms that these amphiphilic conjugates can be used in widespread clinical applications.

Materials and methods

General

Neomycin sulfate, 6-aminohexanoic acid, N-methylmorpholine (NMM), N-hydroxysuccinimide (NHS), 3-(4,5-dimethylthiazol-2-yl)-2,5-diphenyltetrazolium bromide (MTT), Tris, ethidium bromide (EtBr), curcumin, propidium iodide (PI), iodonitrotetrazolium chloride and fluorescein isothiocyanate (FITC) were procured from Sigma-Aldrich Chemical Co., USA. Spectra/por dialysis membrane (MWCO 1 kDa) was purchased from Spectrum Labs, USA. Bradford reagent was obtained from Bio-Rad Inc., USA. Lipofectamine 2000 was purchased from Invitrogen, USA. Particle size and zeta potential measurements were carried out on Zetasizer Nano-ZS (Malvern Instruments, UK). GFP reporter gene expression was observed under Nikon Eclipse TE 2000-S inverted microscope (Kanagawa, Japan). Confocal laser scanning microscopy (CLSM) was performed on a Zeiss LSM 510 Meta confocal microscope. Flow cytometry was carried out on Guava-EasyCyte™ Plus Flow Cytometry System, USA. New compounds synthesized in the present study were characterized by UV-VIS, FTIR and ¹H-NMR. UV-VIS spectrophotometry was performed on Cary 60 spectrophotometer (Agilent Inc., USA). FTIR spectra were recorded on a single beam Perkin Elmer (Spectrum BX Series), USA with the following scan parameters: scan range, 4400-400 cm⁻¹; number of scans, 16; resolution, 4.0 cm⁻¹; interval, 1.0 cm⁻¹; unit, %T. ¹H-NMR spectra were recorded on a Bruker Avance 400 MHz instrument with chemical shifts reported in ppm. The experiments were carried out using MilliQ (deionized) water, pH 7.2, filtered through 0.22 μm sterile filters (Millipore, USA). All other reagents and chemicals used in the study were obtained from local vendors.

Cell culture

The cell lines, HEK293, MCF-7 and N2a, were purchased from National Centre for Cell Science (NCCS, Pune, India). The cells were maintained as monolayer cultures in Dulbecco's modified Eagle's medium (DMEM) supplemented with 10% fetal bovine serum (FBS) and 1% antibiotic cocktail of streptomycin and penicillin. The cells were maintained at 37 °C, 5% CO₂ atmosphere and 95% relative humidity.

Microorganisms and growth conditions

Escherichia coli MG1655 (MTCC 1586), *Pseudomonas aeruginosa* (MTCC 741), *Salmonella typhimurium* (MTCC 98), *Bacillus subtilis* (MTCC 121), *Bacillus cereus* (MTCC 430) and *Staphylococcus aureus* (MTCC 740) were grown at 37 °C in Mueller Hinton Broth

prior to their use. The microorganisms were stored at $-70\text{ }^{\circ}\text{C}$ in brain heart infusion broth supplemented with 10% glycerol.

Plasmid purification

The transfection experiments were carried out using the plasmid encoding enhanced green fluorescent protein (EGFP) gene under the cytomegalovirus early promoter gene. The plasmid was transformed into *E. coli* bacterial strain DH5 α . The plasmid DNA (pDNA) was isolated from transformed cultured bacteria using Qiagen Endofree Maxi-Prep kit as per manufacturer's instructions. The purity of the isolated pDNA was checked spectrophotometrically by taking the ratio of UV absorbance at 260/280.

Synthesis protocol

(I) Boc-F Δ F- ϵ Ahx-OH (**1**)

Compound (**1**) was synthesized and characterized following a procedure reported previously from our lab.¹⁹

(II) Boc-F Δ F- ϵ Ahx-Neo (**2**)

To a pre-cooled solution of Boc-F Δ F- ϵ Ahx-OH (2.1 g, 4.0 mmol) and N-methylmorpholine (NMM, 0.43 ml, 4.0 mmol) in dry THF (20 ml) in an ice-salt bath, isobutyl chloroformate (IBCF, 0.57 ml, 4.0 mmol) was added dropwise. After 10 min, a pre-cooled solution of N-hydroxysuccinimide (NHS, 0.525 g, 4.5 mmol) in THF (5 ml) was added and the mixture was stirred till completion of the reaction (as monitored on TLC). Then, an aqueous solution of neomycin sulphate (5.5 g, 6.0 mmol) containing Na₂CO₃ (1.9 g, 18.0 mmol) was added to the reaction mixture. After 12 h, the solvent was concentrated in vacuo and the resulting solution was washed with ethylacetate to remove unreacted peptide. The resulting aqueous solution was subjected to dialysis (cut off 1 kDa) for three days with intermittent change of water. The dialysed solution was lyophilized and a white solid compound (Pep-Neo, **2**) was obtained (~30 % yield). UV analysis: λ_{max} , 275 nm (Δ F); IR (KBr), ν (cm⁻¹): 1648 (CONH), 1040 (C-O), 3368 (-OH). ¹H-NMR (D₂O, 400 MHz) δ (ppm): 7.1-7.4 (m, Ar-H), 3.0-4.2 (m, Neo), 1.4-2.2 (m, 3 x -CH₃, 5 x -CH₂).

Physicochemical characterization

Self-assembled nanostructures were prepared by dissolving Pep-Neo conjugate (1 mg) in 1.0 ml of deionized double distilled water and vortexed for 2-3 min. The resulting solution was kept for 2 h and DLS studies were carried out on a Zetasizer Nano-ZS (Malvern Instruments,

UK). Pep-Neo/pDNA complex was prepared at w/w ratio of 66.6 and incubated for 30 min at room temperature. Mean hydrodynamic diameters of the nanostructures was determined by cumulant analysis using a dynamic light scattering (DLS) instrument. Scattered light was monitored at 173° to the incident beam and the mean hydrodynamic diameter was obtained from the diffusion coefficient using the Stokes-Einstein equation. Data presented is the average value of 20 runs. The zeta potential of the nanostructures was also determined by carrying out 30 runs in triplicates and the averaged values were estimated by Smoluchowski approximation from electrophoretic mobility.

For TEM imaging, grids were prepared by depositing 10 μl solution of Pep-Neo/pDNA complex (at w/w ratio of 66.6), Pep-Neo (1 mg/ml) and Pep-Neo(curcumin) on carbon-coated copper grids with 1% uranyl acetate negative staining and images were observed at an accelerating voltage of 200 kV on HR-TEM (Tecni G2 20 twin, Tecni 200 kV twin microscope).

Loading studies

(a) Loading of hydrophobic dye (Eosin) in Pep-Neo nanostructures

To study the interaction of Pep-Neo with a hydrophobic molecule, eosin dye, 200 μl solution of eosin dye (10 μM) was titrated with increasing concentration (0.1 mg/ml to 1 mg/ml) of Pep-Neo solution (2 μl). On each addition, emission spectrum was recorded in the range of 520-600 nm (emission slit width 2 nm) with excitation at 518 nm (excitation slit width 2.5 nm) using Perkin Elmer LS55 spectrofluorometer, USA.

(b) Loading of curcumin in Pep-Neo nanostructures

To prepare curcumin loaded Pep-Neo nanostructures, 1 ml of Pep-Neo conjugate (1 mg/ml in H_2O) was heated to 90°C for 30 min and cooled to 40°C . To the resulting solution, 22 μl of curcumin (10 mg/ml in DMSO) was added and incubated for 2 h at 40°C . Then the solution was left for 2 h at room temperature. Unloaded Curcumin was removed by centrifugation of the mixture at $1500\times g$ for 1 h. Curcumin loaded Pep-Neo nanostructures were further analysed for size and zeta potential measurement with DLS and morphology with TEM.

Circular Dichroism (CD) studies

To evaluate the orientation change of Pep-Neo nanostructures in methanol/aqueous media, CD spectra of self-assembled peptides were recorded at different concentrations (0% to 50% methanol in water) in the far UV range (220-300 nm) in a rectangular quartz cuvette of path

length 0.5 cm and band width 1 nm at 0.1 nm resolution. Each spectrum was recorded on JASCO J-815 Spectropolarimeter (Jasco Corp., Tokyo, Japan) as an average of three repeated scans in a continuous scanning mode with 100 nm/min scanning speed and response time of 1 second. The contribution of solvent was subtracted from each spectrum.

Preparation of Pep-Neo/pDNA complexes

To prepare Pep-Neo/pDNA complexes, a solution of Pep-Neo (5 mg/ml) was mixed with 1 μ l of pDNA (0.3 μ g/ μ l) at different w/w ratios (40, 50, 58.3, 66.6, 75.0 and 83.3) in 5% dextrose solution (5 μ l) keeping the amount of pDNA constant. The final volume was made up to 20 μ l with water and solutions were incubated at ambient temperature for 30 min before their use in transfection assay.

Electrophoretic mobility shift assay of Pep-Neo/pDNA complexes

In order to determine the amount of Pep-Neo nanostructures required to completely neutralize the negative charge of known amount of pDNA and retard its mobility on agarose gel, an electrophoretic mobility shift assay was carried out. The Pep-Neo/pDNA and Neo/pDNA complexes were formed at w/w ratios of 0.33, 0.66, 1.0, 1.33, 1.66, 2.0, 2.33, 3.33 and 3.3, 6.6, 10.0, 13.3, 16.6, 20.0, 23.3, 33.3, 50.0, respectively, with 0.3 μ g (1 μ l) of pDNA. The complexes were vortexed and incubated at $25 \pm 2^\circ$ C for 30 minutes. The complexes were then mixed with 2 μ l of 10x loading dye (xylene cyanol), loaded on to 0.8% agarose gel pre-mixed with EtBr and electrophoresed at 100 V for 1h. The bands were visualized on UV transilluminator using a Gel Documentation System (Syngene, UK).

In vitro transfection assay and quantitative analysis

To quantify the GFP expression after transfection assay at an individual cell level, fluorescence assisted cell sorting (FACS) analysis was carried out on two cell lines, MCF-7 and N2a. The cells were seeded at 20,000 cells/well in 24-well plates and incubated for 24 h. After attaining \sim 70% confluency, the media was aspirated off and the cells were washed with 1x PBS. Pep-Neo/pDNA complexes (100 μ l) were prepared at w/w ratios of 58.3, 66.6 and 75.0, and Lipofectamine/pDNA complex was prepared as per manufacturer's protocol. These complexes were incubated for 30 min and then diluted with DMEM (300 μ l) followed by gentle addition in the respective wells. The plates were kept in a CO₂ incubator at 37 $^\circ$ C for 3 h followed by replacement of the media by fresh DMEM containing 10% FBS. Post-36 h of transfection, the media was removed, cells washed with 1x PBS (2 x 1 mL), visualized under a fluorescence

microscope and subjected to trypsinization with 1x trypsin-EDTA solution (200 μ l to each well). The cells were centrifuged at 8000 rpm for 5 min at 4 $^{\circ}$ C. Subsequently, the pellet was washed twice with 1x PBS buffer (1 mL) and suspended the cells in 1x PBS buffer. The cell suspension was transferred to FACS cuvettes and the percent GFP expressed in the cells was determined by flow cytometry using Cytosoft Software. The percentage of transfected cells was calculated by determining the statistics of cells fluorescing above the control level, whereas non-transfected cells were used as control. A total of 5000 events were analyzed to produce statistical data.

Cell cytotoxicity assay

In vitro cell cytotoxicity assay of Pep-Neo/pDNA and Lipofectamine/pDNA complexes was performed in HEK293 and N2a cells by MTT colorimetric assay. The transfection experiments were performed in serum free conditions on HEK293 and N2a cells, as described above. Pep-Neo/pDNA complexes were formed at different w/w ratios of 40, 50, 58.3, 66.6, 75.0 and 83.3 and incubated for 30 min. Similarly, Lipofectamine/pDNA complex was formed following manufacturer's protocol. Post-36 h of transfection, 100 μ L of MTT solution (1 mg/ml in media) was added to each well. The cells were kept in CO₂ incubator for 2 h and then the supernatant was removed and formazan crystals were resuspended in 100 μ L of isopropanol containing 0.06 M HCl and 0.5% SDS. The intensity of color was measured spectrophotometrically at 540 nm on an ELISA plate reader. The untreated cells were taken as control with 100 % cell viability. The relative cell viability compared to control was calculated by the formula : $A_{sample} / A_{control} \times 100$.

Hemolytic activity and cell viability of Pep-Neo nanostructures

The hemolytic activity of Pep-Neo conjugate was performed on human erythrocytes. The concentrated human erythrocytes were washed with 1x phosphate buffered saline (pH 7.4) and suspended in PBS.²⁰ Pep-Neo conjugate was serially diluted in 1x PBS making the final concentration from 25 μ M to 500 μ M and added in a 96-well plate followed by addition of 100 μ l of erythrocytes solution. The plate was incubated at 37 $^{\circ}$ C for 1 h and then centrifuged at 1000 g. The supernatant was collected in another 96-well plate and absorbance at 540 nm was measured on an ELISA plate reader. Triton X-100 (0.1%, w/v) was taken as positive control and 1x PBS as negative control. The percent hemolysis was calculated by the formula: $A_{sample} / A_{tritonX-100} \times 100$.

The toxicity of self-assembled nanostructures of Pep-Neo was also determined on HEK293 and N2a cell lines. The cells were cultured at initial cell density of 10^5 cells/well in a 96-well plate at 37 °C in a humidified 5% CO₂ atmosphere. Pep-Neo nanostructures was added onto the cells in final concentration of 134, 168, 196, 224, 252 and 280 μM. The cells were incubated for 36 h. The MTT assay was performed after 36 h, as described above.

Heparin release assay

To find out the stability of Pep-Neo/pDNA complex, it was prepared at w/w ratio of 66.6 (at which the complex exhibited the highest transfection efficiency) and incubated for 30 min. An anionic polysaccharide, heparin, was added in increasing amounts (ranging from ~10 U to 140 U) to the complexes. After incubation for 30 min, the samples were electrophoresed on 0.8% agarose gel at 100 V for 1 h, stained with EtBr and the bands visualized on UV transilluminator (Syngene, UK). The pDNA released from the complexes was quantified densitometrically using Gene Tool Software from Syngene.²¹

DNase I protection assay

To evaluate the capability of Pep-Neo nanostructures to protect the bound pDNA from nucleases, DNase I protection assay was performed at different time intervals.²² The native pDNA and Pep-Neo/pDNA complex at w/w ratio of 10 were incubated at RT for 0.5, 1 and 2 h with 1 μl of DNase I (1U/μl) in a buffer containing 100 mM Tris, 25 mM MgCl₂ and 5 mM CaCl₂. After incubation, 1 μl of EDTA (100 mM) was added and heated at 80 °C for 10 minutes to inactivate DNase I. The reaction mixture was further incubated at RT for 1 h after adding 100 U of heparin to release the protected pDNA from Pep-Neo/pDNA complexes. The reaction mixture was electrophoresed for 1 h at 0.8% agarose gel stained with EtBr and visualized on UV transilluminator using Syngene gel Documentation system. The amount of pDNA released from Pep-Neo/pDNA complexes after treatment with heparin was estimated by densitometry.

Antimicrobial activity

(a) Zone of inhibition assay

The antimicrobial activity of Pep-Neo conjugate was performed by using Kirby-Bauer single disc susceptibility test. The test was performed on three gram negative bacterial strains, viz., *Escherichia coli* MG1655 (MTCC-1586), *Pseudomonas aeruginosa* (MTCC-741), *Salmonella enterica typhimurium* (MTCC-98) and three gram positive bacterial strains, viz., *Bacillus subtilis* (MTCC-121), *Bacillus cereus* (MTCC-430) and *Staphylococcus aureus*

(MTCC-740). Mueller Hinton agar plates were seeded with bacterial culture and then the sterile filter paper discs of 6 mm diameter were placed, which were then soaked with Pep-Neo conjugate (1 mg/disc). The agar plates were subsequently incubated at 37 °C overnight. Double autoclaved Milli-Q water was used as negative control. The results were recorded by measuring the zone of inhibition (using callipers \pm 0.1 mm) around each filter paper discs. All the experiments were carried out in triplicates.

Determination of minimum inhibitory concentration (MIC)

For the quantitative estimation of antibacterial activity, minimum inhibitory concentration (MIC) assay was performed on the above mentioned six bacterial strains using microwell serial dilution method.²³ The minimum inhibitory concentration is the minimum amount of sample required for completely inhibiting the bacterial growth under standard assay condition. Briefly, 30 μ l of mid-log phase bacterial cultures (OD_{600} = 0.3-0.5) were inoculated in 200 μ l of Mueller Hinton Broth in each well and then serially diluted Pep-Neo conjugate (0.1mg/ml-0.02 mg/ml for gram negative bacterial strains and 0.04 mg/ml-0.003 mg/ml for gram positive bacterial strains) was added followed by incubation at 37 °C overnight. As an indicator of bacterial growth, 30 μ l of 0.2 mg/ml iodinitrotetrazolium chloride (INT) was added to each well and incubated at 37 °C for 30 min. The color formation was observed.

Transmission electron microscopy (TEM) of bacteria

E. coli and *B. subtilis* cultures were collected at a concentration of 10^6 CFU/ml in mid-log phase culture and centrifuged at 5000 rpm for 2 min. The pellet was finely resuspended in fresh MHB media. Pep-Neo sample was added to bacterial culture at a 5x concentration of MIC. The treated bacterial cultures were incubated at 37 °C for 1h in shaking incubator followed by washing with 1x PBS twice. The bacterial cell pellet was fixed in 2.5% glutaraldehyde and 4% paraformaldehyde solution in 1x PBS for 2-3 h at RT followed by washing with 1x PBS twice. The bacterial pellets were then dehydrated gradually using a sequential series of ethanol (10%, 20%, 40%, 60%, 80%, 100%) for 15 min at each step.²⁴ The bacterial sample suspended in 80% ethanol were then added on a carbon-coated copper grid and negatively stained with 6% uranyl acetate solution. The morphology of the treated and untreated bacterial specimens was examined using Tecnai G2 20 twin microscope at an accelerating voltage of 200 kV.

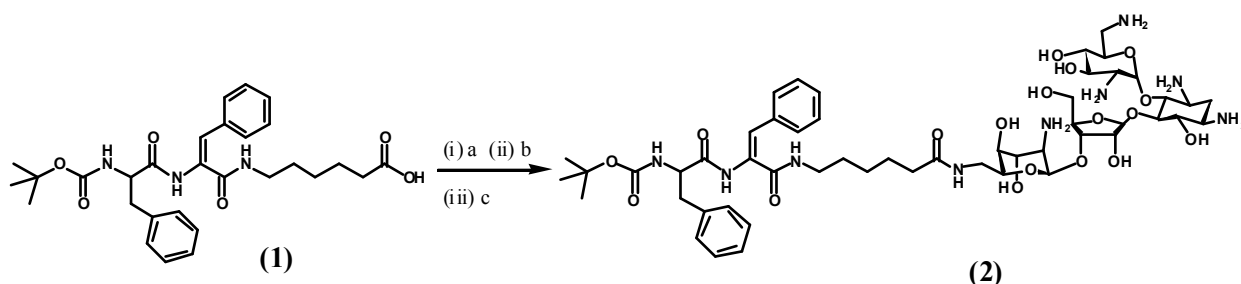
Confocal laser scanning microscopy (CLSM) of treated bacteria

The effect of Pep-Neo nanostructures on bacteria was further studied by observing propidium iodide positive cells using CLSM. The bacterial culture at a concentration of 10^6 CFU/ml was incubated with Pep-Neo at a 2x concentration of MIC for 1h. *E. coli* bacterial culture was then stained with a solution of two dyes, fluorescein isothiocyanate (FITC) and propidium iodide (PI).²⁵ Solution A (5 mg FITC in 1 mL absolute ethanol) and solution B (1 mg PI in 1 ml of PBS) were prepared. The working solution was prepared by mixing 50 μ L of solution A and 40 μ l of solution B in 1.9 ml of 1x PBS. The bacterial suspension was incubated for 30 min at RT on incubator shaker in dark. After incubation, the bacterial suspension was washed with 1x PBS and resuspended in it (1ml). The slides of bacterial samples with cover slips were prepared by putting 5 μ l of bacterial sample on glass slide and air dried. These bacterial slides were then observed under CLSM (Zeiss LSM 510) using a filter set designated for fluorescein and PI. Both the live and dead cells were stained by FITC while only dead cells were stained by PI. To minimize photobleaching, the images were captured at an excitation wavelength of 488 nm first, followed by collecting images of dead cells using an excitation wavelength of 560 nm. Untreated cells were taken as control.

Results and discussion

In the last few years, chemical vectors bearing biocompatibility and biodegradability have attracted more research interest due to their biosafety and ease of preparation. Different types of functional peptides have been designed and developed for in vitro and in vivo delivery of nucleic acids,^{10,26} however, lack of optimum size and cationic charge density for efficient interaction with the genetic material have made it mandatory to conjugate other helper ligands to achieve the optimized property. Recently, some amphiphilic carriers have been developed that self-assemble to generate nanostructures having capability to bind biologically important molecules and mediate their delivery in vitro and in vivo. In one of our previous works, we designed and synthesized an amphiphilic glyco-dehydropeptide that formed stable nanostructures on self-assembly capable of encapsulating hydrophobic molecules but could not get endocytosed through cell membrane due to deficiency of cationic charge at the surface of the nanostructures.¹⁹ Hence, by taking a clue from this study and not only to enhance the cellular uptake of the nanostructures but also the ability to interact with nucleic acids, here, we have conjugated an aminoglycoside, Neomycin, with a modified dehydropeptide. Synthesis of the dehydropeptide, used in the present study, is reported in our earlier publication¹⁹ and conjugation of neomycin is

outlined in scheme 1. Boc-F Δ F- ϵ Ahx-OH (**1**) was first reacted with isobutyl chloroformate to generate mixed anhydride and then with N-hydroxysuccinimide (NHS) to yield active ester, which reacted with amino functions of neomycin (1.5 meq), to produce Boc-F Δ F- ϵ Ahx-Neo conjugate (Pep-Neo, **2**) in ~30% yield after dialysis step. The conjugate was characterized by UV, IR and $^1\text{H-NMR}$ techniques. Absorbance at 275 nm corresponding to dehydrophenylalanine²⁷ confirmed the presence of peptide (**1**) in the conjugate (Figure 1). Further, in IR spectrum, disappearance of a band at 1692 cm^{-1} due to carboxyl function in peptide (**2**) validated the conjugation of neomycin with the peptide (**1**) (Figure 1, inset).



Scheme 1. Schematic representation of synthesis of Pep-Neo (**2**). Reaction conditions: (a) NMM/IBCF, (b) NHS, and (c) Neomycin sulfate /Na₂CO₃

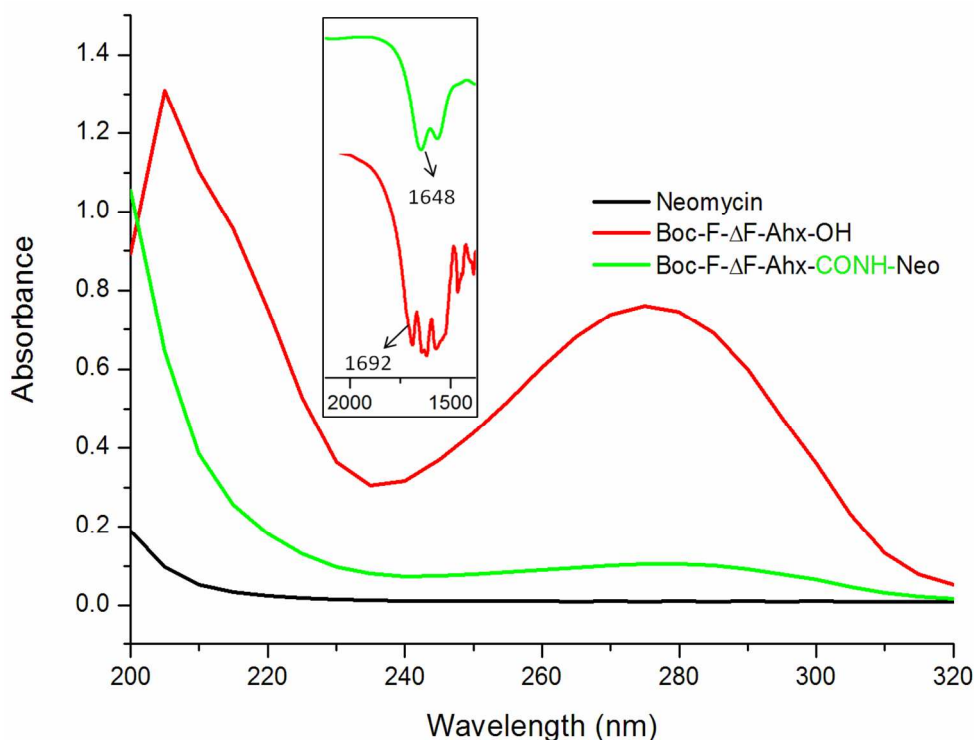


Figure 1. UV Spectra of Neomycin, Boc-F Δ F- ϵ Ahx-OH and Boc-F Δ F- ϵ Ahx-CONH-Neo (Pep-Neo) at equimolar concentration. **Inset** - FTIR spectra of Boc-F Δ F- ϵ Ahx-OH and Boc-F Δ F- ϵ Ahx-CONH-Neo showing conversion of carboxylic group to amide function.

Characterization of Pep-Neo nanostructures

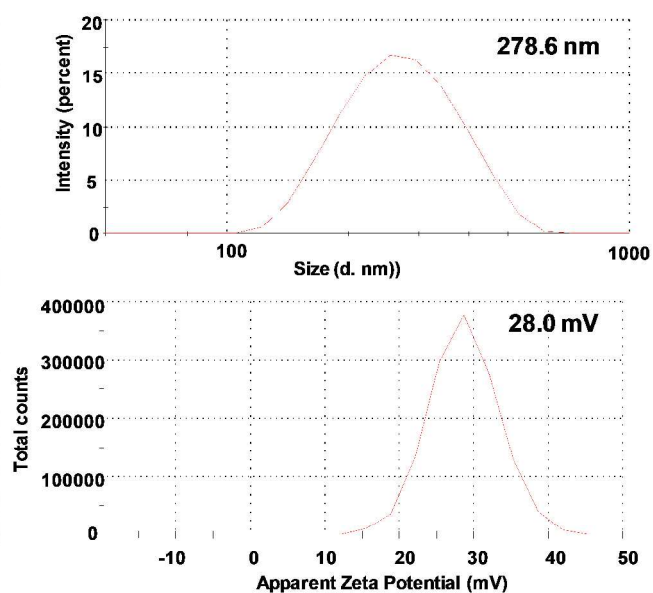
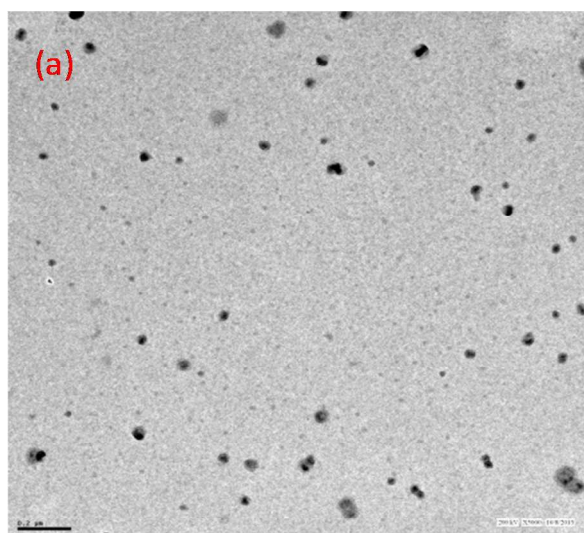
Self-assembly of Pep-Neo conjugate into its nanostructures was studied by DLS. An aqueous solution of Pep-Neo (1 mg/ml) was vortexed and kept for 2h at ambient temperature to form nanostructures, which was then subjected to size measurement. The results revealed that the size of the so formed nanostructures was found to be \sim 279 nm (Table 1). The morphology of these structures was determined by TEM analysis. Figure 2 (a) clearly shows spherical-shaped nanostructures with size \sim 50-70 nm consisting of hydrophilic shell with hydrophobic core. This finding is in agreement with the UV spectroscopic data, wherein the absorbance at 275 nm decreased [*ca.* absorbance of Pep (1) at 275 nm] in case of Pep-Neo (2) due to burial of hydrophobic segment of Pep-Neo conjugate in the core of the nanostructures indicating the non-accessibility for measurement. The difference in the size measured by DLS and TEM might be due to measurement of hydrodynamic diameter in the former, while the later one measures the size of the nanostructures in dry state.¹⁴ In order to further confirm the self-assembly into the nanostructures, i.e. hydrophilic shell with hydrophobic core, a hydrophobic molecule, curcumin, was encapsulated. DLS study showed a significant decrease in the particle size from 279 nm to \sim 85 nm (Table 1) suggesting the incorporation of curcumin in the hydrophobic core via hydrophobic interactions, which resulted in the compactness of the nanostructures.¹⁹ Similarly, TEM analysis showed a decrease in the size of the curcumin-entrapped nanostructures in the range of 35-50 nm (Figure 2c). These results advocate the potential of these nanostructures to encapsulate hydrophobic molecules.

Zeta potential measurements were also carried out of the Pep-Neo nanostructures, which was found to be \sim +28 mV, whereas the curcumin-encapsulated nanostructures showed \sim +16 mV (Table 1). This could be due to formation of more compact structures, which restricted the accessibility of total charge. Further, these nanostructures were allowed to interact with the plasmid DNA (pDNA) and the results showed a decrease in size and zeta potential of the complex (i.e. \sim 154 nm and \sim +19 mV). In the presence of serum (10% FBS), both the parameters displayed a further decrease (i.e. size \sim 114 nm and zeta potential \sim -8 mV), which could be due to adsorption of serum proteins on the cationic surface inhibiting aggregation among the

nanostructures as well as absorption of water by the serum proteins causing partial dehydration around the complexes that resulted in the compaction of the size of the nanostructure complexes.²⁸⁻³⁰ Pep-Neo/pDNA complex was also analyzed by TEM, where the size was obtained in the range of 40-60 nm (Figure 2b).

Table 1. Size and zeta potential measurements of Pep-Neo, Pep-Neo(Curcumin) and Pep-Neo/pDNA complex (at w/w ratio of 66.6)

S.No.	Sample	Average particle size (d. nm) \pm S.D.	PDI \pm S.D.	Zeta potential (in mV) \pm S.D.
1	Pep-Neo (in H ₂ O, 1mg/ml)	278.6 \pm 6.55	0.329 \pm 0.047	28.0 \pm 0.62
2	Pep-Neo /pDNA complex (in H ₂ O)	154.4 \pm 4.55	0.103 \pm 0.032	19.4 \pm 1.29
3	Pep-Neo/pDNA complex (in 10% FBS)	113.7 \pm 0.56	0.607 \pm 0.0014	-7.51 \pm 0.46
4	Pep-Neo(Curcumin) (in H ₂ O, 1mg/ml)	85.37 \pm 1.32	0.124 \pm 0.012	16.4 \pm 0.75



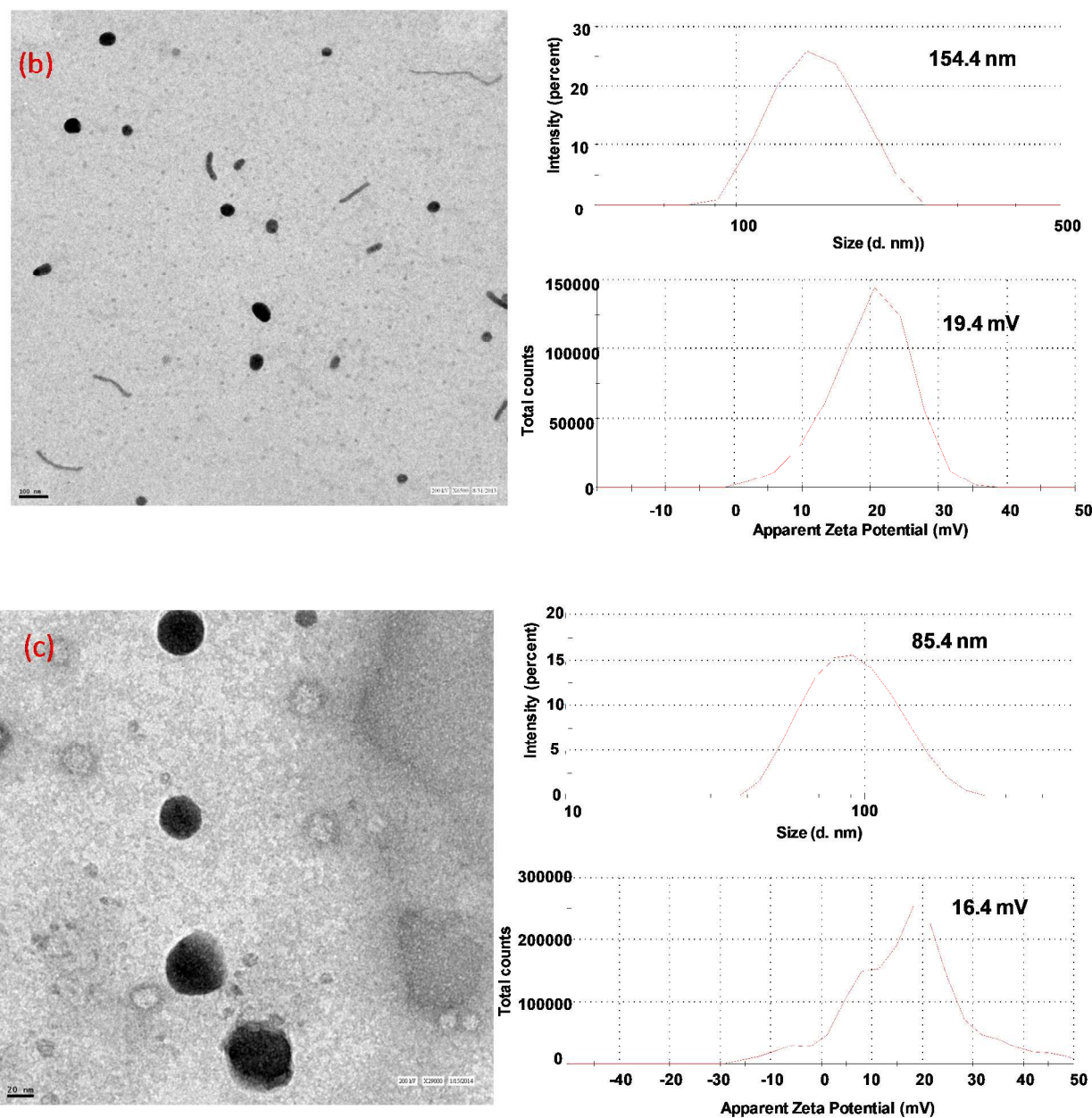


Figure 2. TEM images of (a) Pep-Neo (in H₂O), scale bar: 0.2 μ m, (b) Pep-Neo/pDNA complex (at w/w ratio of 66.6 in H₂O), scale bar: 100 nm, and (c) Curcumin-entrapped Pep-Neo nanostructures, scale bar: 20 nm.

Effect of concentration and pH on the size and zeta potential of the Pep-Neo nanostructures

In order to examine the effect of concentration, we have carried out size and zeta potential measurements of Pep-Neo nanostructures at different concentrations (0.5, 1.0, 2.5 and 5

mg/ml). The results revealed that change in the concentration did not show significant change in the size of the nanostructures. It varies from 282 nm to 299 nm. However, a difference in the zeta potential measurements was observed, i.e. on increasing the concentration of the nanostructures in water, zeta potential changed from 31.6 mV (0.5 mg/ml) to 23.2 mV (5 mg/ml), which might be explained on the basis that on increasing the concentration, more compactness in the structure was observed (Table 2).

Table 2. Effect of concentration on the size and zeta potential of Pep-Neo nanostructures

S.No.	Sample	Average particle size nm \pm S.D.	PDI \pm S.D.	Zeta potential mV \pm S.D.
1	Pep-Neo (5 mg/mL)	299.4 \pm 6.684	0.423 \pm 0.056	23.2 \pm 0.404
2	Pep-Neo (2.5 mg/mL)	294.7 \pm 1.401	0.373 \pm 0.036	25.5 \pm 1.0
3	Pep-Neo (1 mg/mL)	281.6 \pm 8.701	0.392 \pm 0.044	28.7 \pm 1.35
4	Pep-Neo (0.5 mg/mL)	294.4 \pm 8.707	0.474 \pm 0.095	31.6 \pm 2.25

Similarly, effect of change in the pH was investigated on the size and zeta potential of the nanostructures. The measurements were carried out at three different pHs (5.5, 7.0 and 8.5). On changing pH of the medium, nanostructures showed a significant change in their size and zeta potential. Table 3 shows that at pH 7.0, the size and zeta potential of Pep-Neo nanostructures were found to be \sim 282 nm and 28.7 mV, respectively. On changing the pH from 7.0 to 8.5, no significant changes were observed, however, on decreasing the pH from 7.0 to 5.5, the size and zeta potential of the nanostructures increased significantly to \sim 483 nm and 43.5 mV, respectively. This could be due to the protonation of the amines present in nanostructures which resulted in the repulsion within the ammonium ions leading to increase in the size of nanostructures and these cationic ammonium ions showed an increase in zeta potential value of these nanostructures.³¹

Table 3. Effect of pH on the size and zeta potential of Pep-Neo nanostructures

S.No.	Sample	Average particle size nm \pm S.D	PDI \pm S.D.	Zeta potential mV \pm S.D.
1	Pep-Neo (pH 5.5)	482.9 \pm 77.34	0.558 \pm 0.10	43.5 \pm 2.11
2	Pep-Neo (pH 7.0)	281.6 \pm 8.701	0.392 \pm 0.044	28.7 \pm 1.35
3	Pep-Neo (pH 8.5)	284.18 \pm 13.97	0.375 \pm 0.060	29.6 \pm 2.32

Loading studies

For development of a new efficient self-assembled nanostructures as delivery vehicles, loading of molecules in these structures is the main requirements. Formation of these nanostructures with the help of different types of weak interactions is yet to be understood. In the aqueous media, the aggregation process is predominantly driven by the hydrophobic interactions. It would be interesting to monitor the assembly process using loading of hydrophobic molecules such as eosin and curcumin. Here, we have evaluated the interaction of cationic amphipathic peptide, Pep-Neo, with a hydrophobic molecule, eosin. On addition of Pep-Neo conjugate to eosin (10 μ M), we started recording the emission spectra from 520-600 nm before and after addition of the conjugate. Initial addition of Pep-Neo (0.1 mg/ml) quenched the fluorescence of eosin, while a red shift was observed later followed by intensity enhancement as concentration of Pep-Neo increased. The results are in agreement with the reported literature³² suggesting that the conjugate quenched the fluorescence of eosin in its pre-micellar region due to extensive π - π stacking and electrostatic interaction between amphiphilic conjugate and eosin (Figure 3). Hydrophobic part of Pep-Neo consists of Boc-F Δ F- ϵ Ahx-, which interacts with planar aromatic structure of eosin eventually leading to fluorescence quenching.¹⁹ These results, therefore, suggested that loading of eosin occurred via hydrophobic interactions between eosin molecules and hydrophobic moiety in Pep-Neo nanostructures. Similarly, another hydrophobic molecule, curcumin, was encapsulated in the nanostructures, which was confirmed by DLS and electron microscopic analysis, as discussed above (Table 1 and Figure 2c).

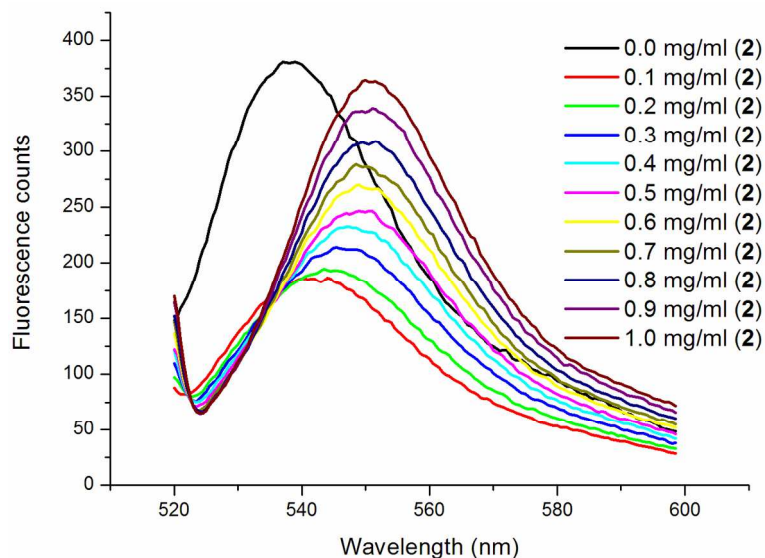


Figure 3. Emission spectra of eosin (10 μ M) recorded with increasing concentration of Pep-Neo (2)

CD studies

Loading of a cargo molecule can be achieved through interaction with the constituent molecules in the nanostructure. In the present study, nanostructures of Pep-Neo has cinnamoyl moiety ($-\text{C}_6\text{H}_5-\text{C}=\text{C}-\text{C}=\text{O}$) in dehydro-Phe amino acid residue, which exhibits a characteristic CD band at 275 nm due to charge transfer electronic transition from electron donating styryl group to the electron accepting carbonyl group that strongly depends on the peptide conformation. The molar ellipticity of the peptide in this region depends on its conformation.^{27,33} Therefore, the CD band in this region of dehydro-Phe containing peptides can serve as a sensitive conformation probe to follow the change in interaction of self-assemblies having dehydro-Phe residues.^{23,28} CD spectra of Pep-Neo (1.0 mg/ml) were recorded in water containing different %age of methanol in UV range (220-320 nm). Change in molar ellipticity was monitored as a function of methanol/water ratio. On increasing the methanol concentration from 0-50%, the CD spectrum changed, which indicated that Pep-Neo molecules have different orientations in these media, as also observed in DLS studies with different average sizes and surface charges of nanostructures (Figure 4 and Table 4). From 0-10% methanol, the average size of nanostructures decreased, however, further increase in methanol content, the average size increased. In case of surface charge measurements, the charge on these nanostructures

decreased with an increase in the amount of methanol in water. The DLS data supported the different orientations of Pep-Neo in these nanostructures.

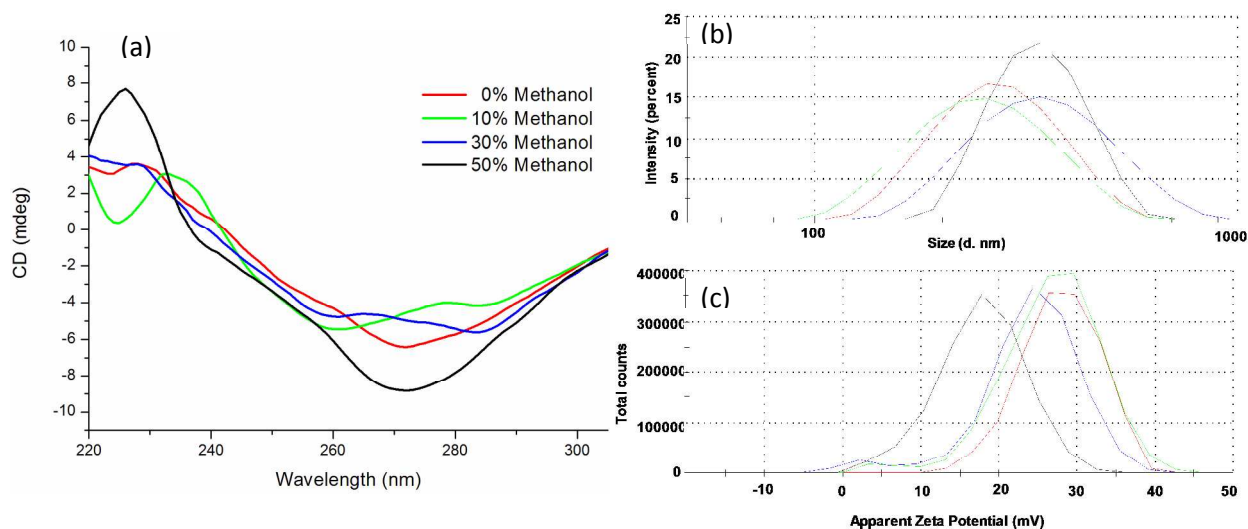


Figure 4. (a) CD spectra of Pep-Neo nanostructures in different composition of methanol/water, (b) and (c) change in the size and zeta potential of nanostructures with increasing methanol percentage in water, respectively.

Table 4. Size and zeta potential measurements of Pep-Neo nanostructures on increasing methanol composition in water

S.No.	Pep-Neo (1 mg/ml)	Average size (d. nm) \pm S.D.	PDI \pm S.D.	Zeta potential (mV) \pm S.D.
1.	Water	278.6 \pm 6.6	0.329 \pm 0.047	28.0 \pm 0.6
2.	10% Methanol	241.0 \pm 3.7	0.206 \pm 0.007	27.2 \pm 0.6
3.	30% Methanol	312.5 \pm 3.6	0.165 \pm 0.017	23.2 \pm 0.7
4.	50% Methanol	332.1 \pm 9.4	0.144 \pm 0.024	17.6 \pm 0.2

Electrophoretic mobility shift assay

The binding ability of Pep-Neo nanostructures to negatively charged pDNA was assessed by agarose gel electrophoresis. Pep-Neo/pDNA complexes were prepared at various w/w ratios ranging from 0.33 to 3.33 and similarly, Neomycin/pDNA complexes were prepared at w/w ratios from 3.3 to 50. The results are depicted in figure 5, where it was observed that Pep-Neo nanostructures could retard the mobility of pDNA at w/w ratio of 3.33 indicating complete

condensation of pDNA at this weight ratio. On the other hand, neomycin could hardly show condensation of pDNA even at w/w ratio of 50, although it also carries cationic charge. The results demonstrate that self-assembly into nanostructures of Pep-Neo conjugate plays an important role in localization of cationic charge density required for pDNA binding.

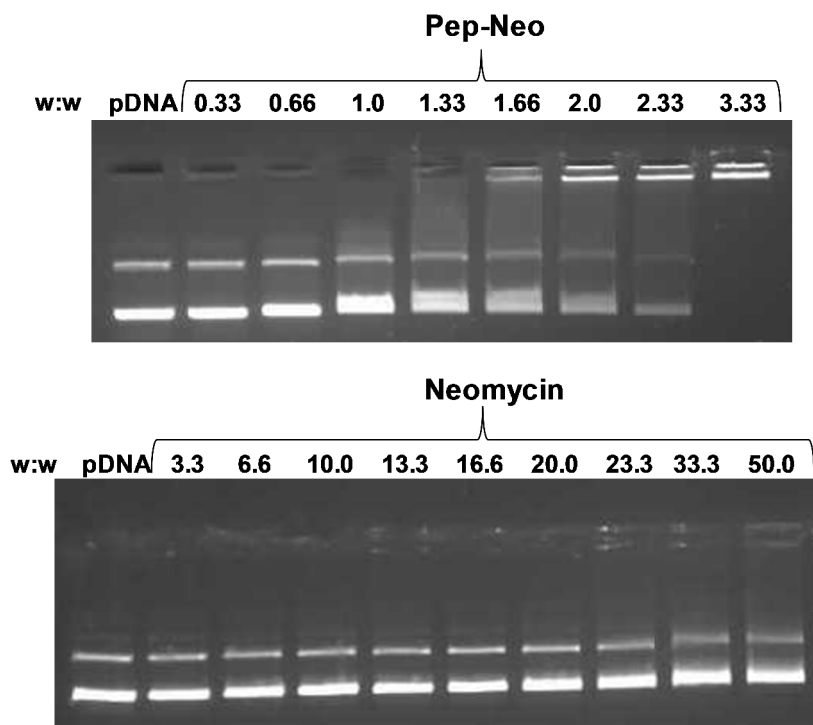


Figure 5. Gel retardation assay of Pep-Neo/pDNA and neomycin/pDNA complexes. Pep-Neo nanostructures and neomycin were complexed with 0.3 μg of pDNA at different w/w ratios. After 30 minutes of incubation, complexes were electrophoresed on 0.8% agarose gel at 100 V for 1h.

Heparin release assay

DNA binding ability of the nanostructures was determined by gel retardation assay, however, to examine the stability of Pep-Neo/pDNA complex, heparin release assay was carried out to mimic intracellular disassembly of the complex. An efficient cationic vector is required to bind pDNA, carry it inside the cells and release it quantitatively at the target site for necessary processing. It is an important factor which governs the efficacy of the vector. Figure 6 shows the pDNA release pattern from the nanostructures post-heparin treatment followed by densitometric analysis of the bands on agarose gel. Pep-Neo/pDNA complex released $\sim 60\%$ pDNA with ~ 20 U of heparin, while increasing the amount of heparin, $\sim 72\%$ pDNA was released with 48 U indicating optimum stability of the complex.

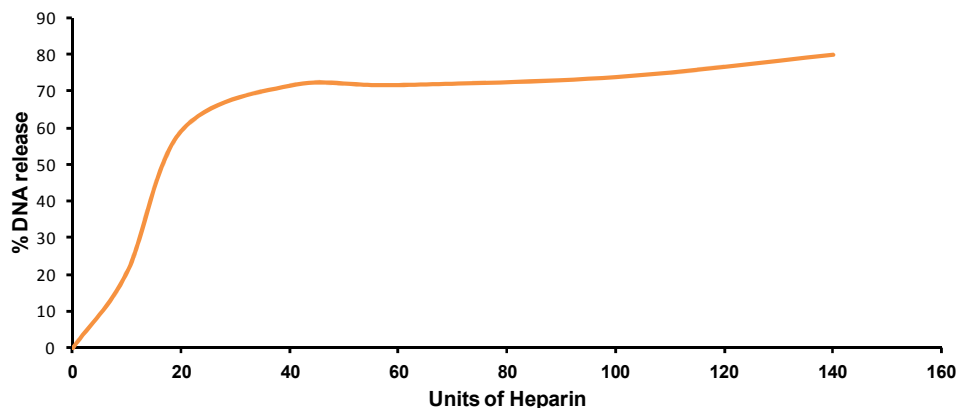


Figure 6. pDNA release assay of Pep-Neo/pDNA complex. To 20 μ l of Pep-Neo/pDNA complex (w/w 66.6), heparin was added in increasing amounts and incubated for 30 min at RT. The samples were run on EtBr-stained 0.8% agarose gel at 100 V for 1 h. Quantification was done by densitometry.

Enzymatic assay

For a gene delivery system to be effective, the protection of pDNA from nucleases present in the cellular environment is a prerequisite as native pDNA is prone to degradation by nucleases. Here, it was observed that free pDNA was completely degraded by nucleases in 30 minutes while pDNA complexed with Pep-Neo remained intact (upto 90%) even after 2 h of incubation with DNase I (Figure 7). These observations suggest that Pep-Neo can be used as an effective carrier for therapeutic genes.

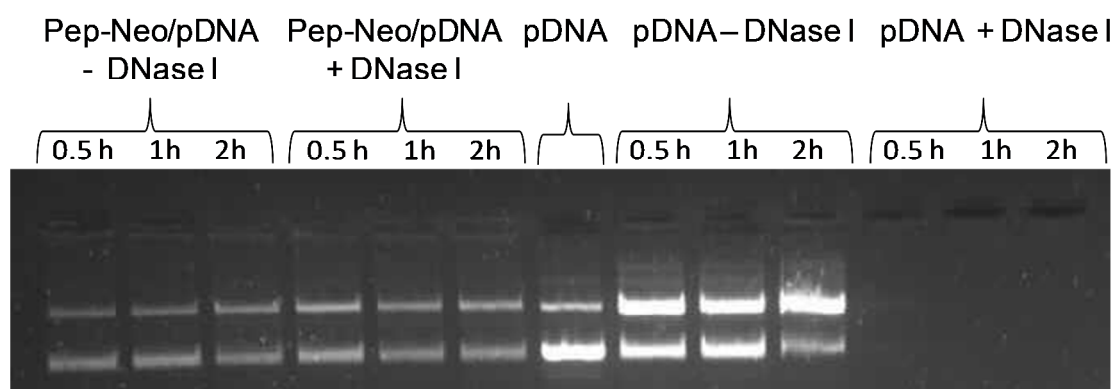


Figure 7. DNase I protection assay of Pep-Neo/pDNA complex. The complex and native pDNA were treated with DNase I for different time intervals. pDNA was released from treated complex by addition of heparin. The amount of pDNA protected was calculated by relative integrated densitometry analysis, quantified and normalized by pDNA values using Gel Documentation system Syngene UK.

In vitro transfection assay and quantification by flow cytometry

In order to evaluate the capability of Pep-Neo nanostructures to transfer nucleic acids inside the cells, gene transfection assay was performed on MCF-7 and N2a cells in 24-well plates. After preliminary examination, final transfection assay was performed using Pep-Neo/pDNA complex at w/w ratios of 58.3, 66.6 and 75.0. Lipofectamine/pDNA complex was prepared following the manufacturer's protocol and used as the standard for comparison purposes. As transfection efficiency depends on the cell type as well as w/w ratio, we observed different pattern of gene expression in both the cell lines varying with w/w ratios. Of the two cells, MCF-7 displayed higher transfection efficiency than that observed in N2a cells. In MCF-7 cells, Pep-Neo/pDNA complex exhibited transfection in ~27% cells at w/w ratio of 66.6, while the standard, Lipofectamine/pDNA complex, could transfect only ~15% cells (Figure 8). Pep-Neo/pDNA complex at w/w ratio of 58.3 and 75 showed higher transfection than Lipofectamine/pDNA complex. Higher transfection efficiency displayed by Pep-Neo/pDNA complex might be due to various factors such as size of the complexes, surface charge on the complexes, higher uptake and easy disassembly of the complex inside the cells. Size and surface charge play an important role in the uptake of the complexes into the cells.³⁴ It is well established that smaller sized complexes are efficiently taken up by the cells and easily internalized, while surface charge not only facilitates interactions with the cell membrane but also helps in the endosomal escape. Besides, hydrophobicity further assists in the release of the complexes from the endosomal compartment by interaction with the endosomal membrane. pH studies carried out in the present investigation also supports this finding as at pH 5.5, the nanostructures displayed disassembly, which resulted in an increase in the zeta potential leading to easy release of the complex in the cytoplasm for nuclear localization. However, in N2a cells, a hard to transfect cell line, Pep-Neo/pDNA complex transfected 7.5-10% cells at different w/w ratios compared to 12.5% cells transfected by Lipofectamine/pDNA complex (Figure 8).

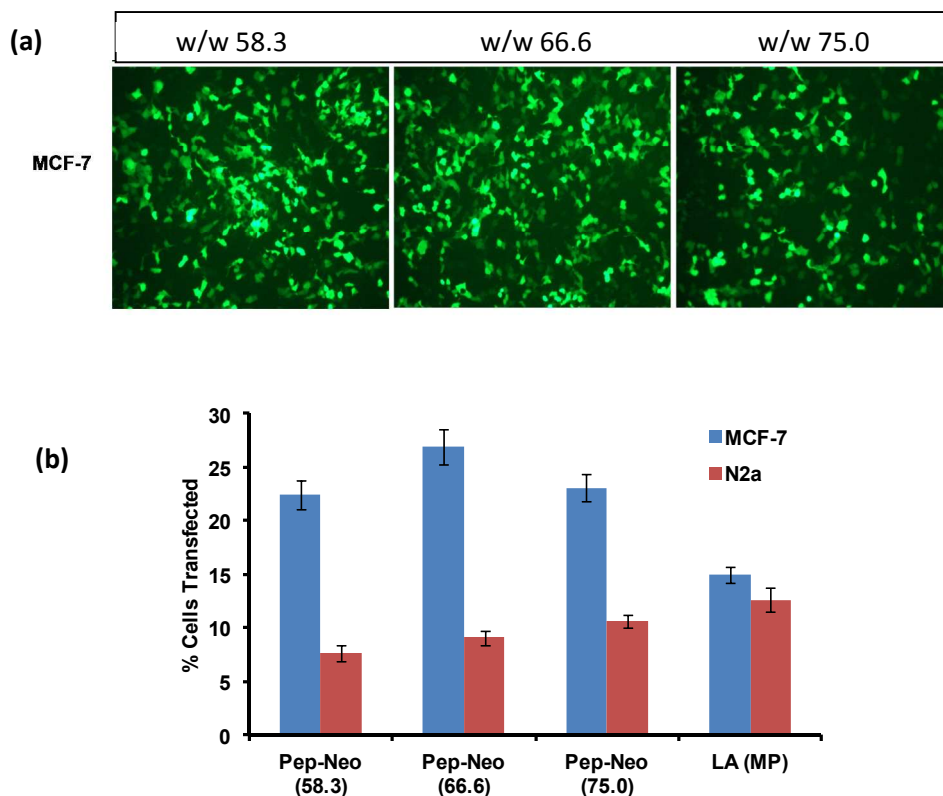


Figure 8. Transfection efficiency of Pep-Neo/pDNA complex: (a) fluorescence microscopic images of GFP expression at different w/w ratios in MCF-7 cells, and (b) quantification of GFP expressed cells, evaluated by FACS, in MCF-7 and N2a cells.

Cytotoxicity

Cytotoxicity of chemical vectors is one of the major areas of concern for developing gene delivery vectors. For safe and efficient transfection, the vector should be non-toxic to cells. Cationic synthetic polymers are well known to destabilize cell membrane and ultimately rupture it due to strong electrostatic interactions between the amine groups of the polymers and cellular compartments, or accumulation of non-degraded polymers in the cell. Therefore, to examine the cytotoxicity of Pep-Neo nanostructures in vitro, N2a and HEK293 cells were transfected with Pep-Neo/pDNA complexes at various w/w ratios. Cells treated with Pep-Neo/pDNA complexes were found to be ~65-92% viable (Figure 9). Of the two cell lines, cell viability was higher in case of HEK293 cells. Lipofectamine/pDNA complex was used for comparison, which showed cell viability in the range of ~60-70% in N2a and HEK293 cells. Pep-Neo/pDNA complex displayed a gradual decrease on increasing w/w ratio of the complex, which might be due to an increase in the amount of Pep-Neo nanostructures in the complex.

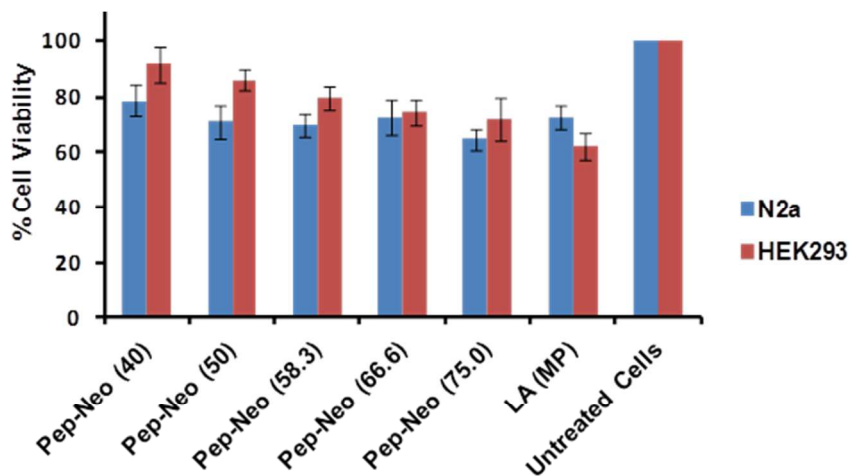


Figure 9. Cell viability of Pep-Neo/pDNA complexes at various w/w ratios and Lipofectamine (LA)/pDNA complex on HEK293 and N2a cells

Hemolytic activity and cell viability of Pep-Neo nanostructures

Hemolysis is one of the major side effects caused by many cationic peptides. Due to their amphipathic nature, these peptides interact with the cell membrane and display a certain degree of hemolytic activity.³⁵ To assess the hemolytic activity of the Pep-Neo nanostructures, we tested these in the concentration range of 10-500 μM for their cytotoxicity to human red blood cells. It was observed that in the tested range, these nanostructures did not show notable hemolysis effect (Figure 10a) compared to Triton-X 100, which exhibited 100% lysis of hRBCs.

Similarly, toxicity of these nanostructures was evaluated on N2a and HEK293 cells at various concentrations (134-280 μM) using MTT assay. It was observed that within this range, the nanostructures showed ~70-90% cell viability on both the cell lines suggesting the non-toxic nature of the projected Pep-Neo nanostructures (Figure 10b). These results ensure that the nanostructures can be used effectively as potential antimicrobial agents with almost negligible toxicity.

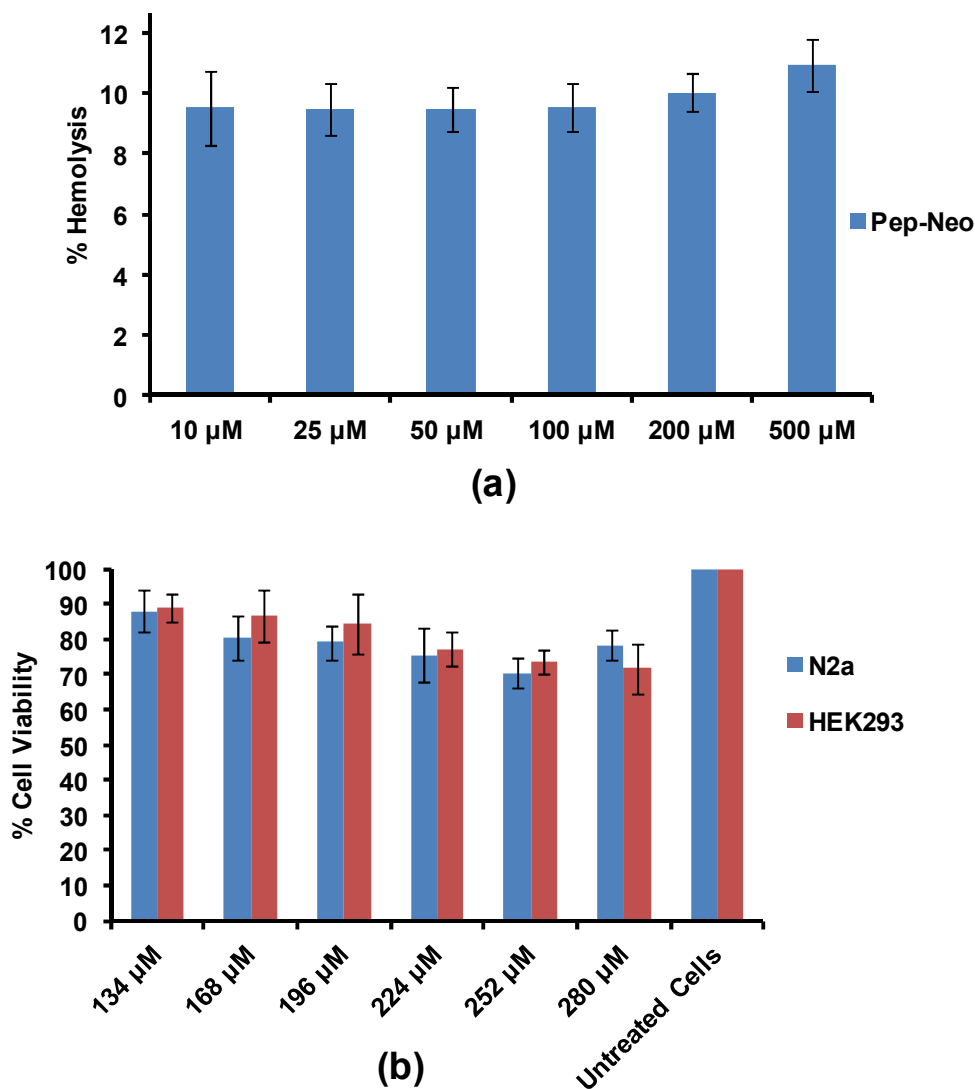


Figure 10. (a) Percent hemolysis assay, and (b) cell viability assay of Pep-Neo nanostructures at different concentrations on N2a and HEK293 cells post-36h of incubation.

Antimicrobial Activity of Pep-Neo nanostructures

Antimicrobial peptides are being used as promising and potential drug molecules for various biomedical applications due to their broad range of activity, low cytotoxicity and decreased resistance development by target cells.³⁶ To exhibit their antibacterial activities, various factors such as charge, size, amphipathic stereo-geometry, hydrophobicity, and peptide self-association to the biological membrane contribute significantly.³⁷ Size of the peptides considerably affects the diffusion and secretion of peptide outside the cells, which is a major factor for eliciting immediate defense response against pathogenic microbes.³⁸ In the present study, the amphiphilic peptide conjugate assembles into nanostructures with a core-shell

structure, where peptide segment forms a hydrophobic core and the cationic neomycin moiety forms a hydrophilic shell, which faces the exterior. As expected, the hydrophobic inner core and cationic outer surface of Pep-Neo self-assembled nanostructures may lead to greater electrostatic interactions with the bacterial membranes, which in effect translate into antimicrobial activity. We evaluated antimicrobial and cell lytic effect of Pep-Neo nanostructures on the bacteria. For this purpose, we selected three gram negative bacterial strains i.e. *E. coli*, *P. aeruginosa*, *S. typhimurium* and three gram positive bacterial strains i.e. *B. subtilis*, *B. cereus* and *S. aureus*. The antibacterial activity of Pep-Neo was evaluated against different test organisms using water as control. The results showed that the Pep-Neo nanostructures retained the antimicrobial activity against both gram positive and gram negative strains and unlike neomycin, which is effective against gram negative strains,³⁹ here, these nanostructures showed higher activity in gram positive bacteria (Table 5).

Table 5. Antibacterial activity (zone inhibition and MIC in $\mu\text{g/ml}$) of Pep-Neo nanostructures against various gram negative and gram positive bacterial strains

Organisms	Zone of inhibition (mm) \pm S.D	MIC (in $\mu\text{g/mL}$)
<i>B. subtilis</i>	12.66 \pm 0.57	9
<i>B. cereus</i>	15.33 \pm 2.30	8
<i>S. aureus</i>	13.33 \pm 1.53	8
<i>E. coli</i>	13.00 \pm 1.41	60
<i>P. aeruginosa</i>	15.00 \pm 1.0	70
<i>S. typhimurium</i>	10.66 \pm 2.08	40

Further, to understand the mechanism of the antimicrobial function of the projected nanostructures, we investigated morphological changes of various microorganisms before and after incubation with the synthesized Pep-Neo nanostructures at 5x MIC for 1 h through transmission electron microscopy (TEM). Untreated *E. coli* and *B. subtilis* exhibited a smooth surface, while treated ones showed broken cell wall, which leads to cell death suggesting efficient interactions of Pep-Neo nanostructures with the cell wall (Figure 11).

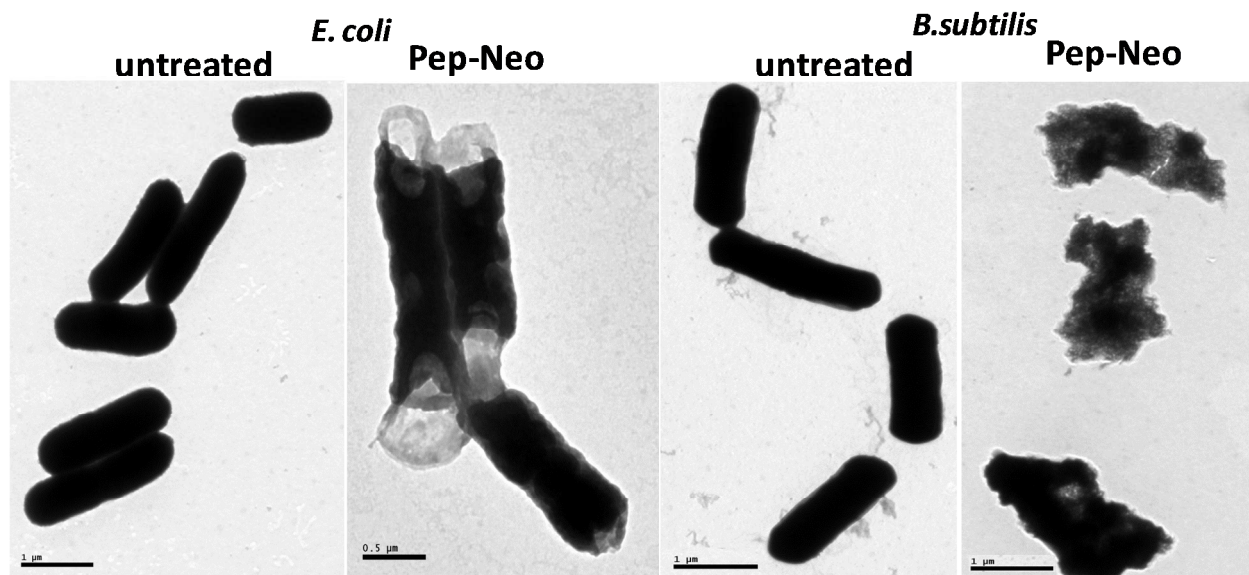


Figure 11. TEM images of untreated and Pep-Neo treated *E. coli* and *B. subtilis*

Although the detailed mechanism has not been determined for antimicrobial peptides, all the evidences suggest that all members of these peptide family penetrate freely through the membrane of Gram-negative bacteria into the periplasmic space, prior to dispersion in the cells.⁴⁰ The latter step may involve an active transport process. In order to determine the viability of bacteria in the presence of Pep-Neo nanostructures, we performed confocal laser scanning microscopy (CLSM) by staining bacteria with fluorescein isothiocyanate (FITC) and propidium iodide (PI).²⁵ FITC stains bacterial cell wall by forming covalent linkage with proteins, while PI specifically stains dead bacteria by interacting with nucleic acids of the compromised cell membrane. Uptake studies of Pep-Neo nanostructures were carried out on Gram-negative bacteria, *E. coli*. After 1h of treatment with 2x MIC concentration, staining of treated and untreated bacteria was performed with two dyes (FITC and PI). The slides of bacterial samples with cover slips were prepared and imaging was done at different wavelengths, i.e. 488 nm for FITC and 560 nm for PI. The images of untreated and treated *E. coli* are shown in figure 12. All bacteria (live and dead) were stained green, whereas only dead bacteria were stained red and yellow sites in images show dead cells by merging of both the images. Images captured at 488 nm and 560 nm clearly show the antimicrobial behavior of Pep-Neo nanostructures.

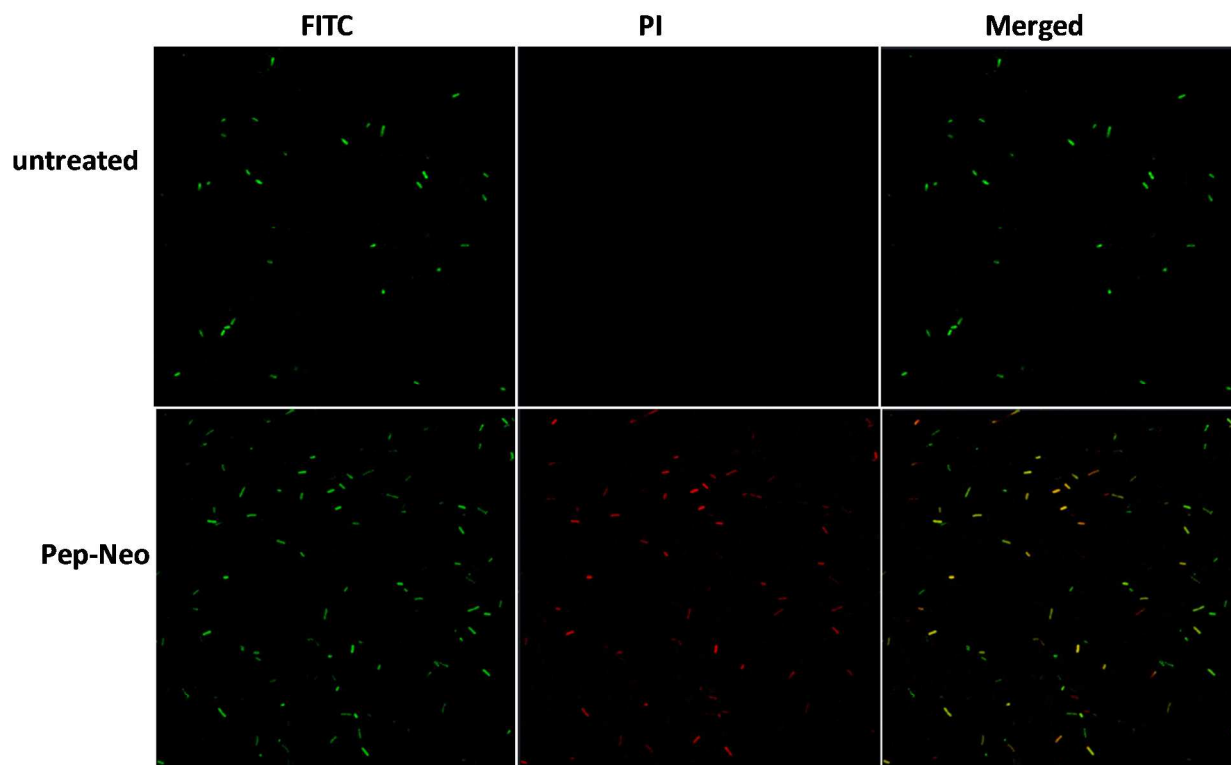


Figure 12. Confocal images of *E. coli* untreated and treated with Pep-Neo nanostructures. In both the series, green dots represent live and dead *E. coli*; red dots in the middle represent dead *E. coli*; yellow dots represent dead *E. coli* and green dots are alive ones.

Conclusions

We have developed a multifunctional amphiphilic conjugate (Pep-Neo) of a hydrophobic modified dipeptide (Boc-F Δ F- ϵ Ahx) segment and hydrophilic cationic aminoglycoside, neomycin, which self-assembles to form nanostructures of defined size and bears sufficient accumulated charge density capable of interacting with pDNA and cell membranes. These nanostructures efficiently condensed GFP encoding pDNA and exhibited significantly higher transfection efficiency in vitro. These structures also showed capability to encapsulate hydrophobic drugs in the peptide core. Besides, these nanostructures displayed antimicrobial activity in gram positive and gram negative bacteria with minimal toxicity. Altogether, these results advocate the promising potential of these biodegradable and biocompatible nanostructures as multifunctional carrier of nucleic acids capable of delivering drugs and controlling bacterial infection simultaneously in future biomedical applications. It would be interesting to study the

multifunctional activities of guanidino and modified guanidino-Pep-Neo conjugates, which is currently under investigation in our laboratory.

Acknowledgements

Financial support from the CSIR-network Project, BSC0120, is gratefully acknowledged. Authors, MM and SRD, also thank UGC and DST (GAP0104) for financial grants to carry out the present work. We are grateful to Mr. Mahendra Pratap Singh, CSIR-IGIB, for carrying out TEM analysis.

References

- 1 (a) U. L. Witz and A. Gopferich, *Eur. J. Pharm. Biopharm.*, 2005, **60**, 247–266; (b) S. Y. Wong, J. M. Pelet and D. Putnam, *Prog. Polym. Sci.*, 2007, **32**, 799–837; (c) M. S. Al-Dosari and X. Gao, *AAPS*, 2009, **11**, 671–681; (d) H. Parhiz, W. T Shier and M. Ramezani, *Int. J. Pharm.*, 2013, **457**, 237-259; (e) S. P. Chaplot and I. D. Rupenthal, *J. Pharm. Pharmacol.*, 2014, **66**, 542-556; (f) L. Jin, X. Zeng, M. Liu, Y. Deng and N. He, *Theranostics*, 2014, **4**, 240-255.
- 2 (a) Q. Liu, C. Wang, Y. Cao, X. Xu and L. Zhang, *J. Mater. Chem. B*, 2014, **2**, 933-944; (b) S. K. Tripathi, V. P. Singh, K. C. Gupta and P. Kumar, *J. Mater. Chem. B*, 2013, **1**, 2515-2524; (c) M. Arif, S. K. Tripathi, K. C. Gupta and P. Kumar, *J. Mater. Chem. B*, 2013, **1**, 4020-4031; (d) R. Bansal, S. K. Tripathi, K. C. Gupta and P. Kumar, *J. Mater. Chem.*, 2012, **22**, 25427-25436.
- 3 (a) J. C. Rea, R. F. Gibly, A. E. Barron and L. D. Shea, *Acta Biomater.*, 2009, **5**, 903-912; (b) H. Margus, K. Padari and M. Pooga, *Mol. Ther.*, 2012, **20**, 525–533; (c) I. Nakase, G. Tanaka and S. Futaki, *Mol. BioSyst.*, 2013, **9**, 855-861; (d) R. M. Levine, C. M. Scott and E. Kokkoli, *Soft Matter*, 2013, **9**, 985-1004.
- 4 J. G. Duguid, C. Li, M. Shi, M. J. Logan, H. Alila, A. Rolland, E. Tomlinson, J. T. Sparrow and L. C. Smith, *Biophys. J.*, 1998, **74**, 2802-2814.
- 5 W. J. Yi, J. Yang, C. Li, H. Y. Wang, C. W. Liu, L. Tao, S. X. Cheng, R. X. Zhuo and X. Z. Zhang, *Bioconjugate Chem.*, 2012, **23**, 125–134.
- 6 C. Wang, L. Ning, H. Wang, Z. Lu, X. Li, X. Fan, X. Wang and Y. Liu, *Int. J. Nanomedicine*, 2013, **8**, 3631-3640.
- 7 W. Qu, S. Y. Qin, Y. Kuang, R. X. Zhuo and X. Z. Zhang, *J. Mater. Chem. B*, 2013, **1**, 2147-2154.

- 8 J. X. Chen, X. D. Xu, S. Yang, J. Yang, R. X. Zhuo and X. Z. Zhang, *Macromol. Biosci.* 2013, **13**, 84-92.
- 9 R. Ischakov, L. Adler-Abramovich, L. Buzhansky, T. Shekhter and E. Gazit, *Bioorg. Med. Chem.*, 2013, **21**, 3517-3522.
- 10 H. Tsutsumi and H. Mihara, *Mol. BioSyst.* 2013, **9**, 609-617.
- 11 F. Shima, T. Akagi, T. Uto and M. Akashi, *Biomaterials*, 2013, **34**, 9709-9716.
- 12 P. Loyer, W. Bedhouche, Z. W. Huang and S. Cammas-Marion, *Int. J. Pharm.*, 2013, **454**, 727-737.
- 13 G. Fichman and E. Gazit, *Acta Biomater.* 2014, **10**, 1671-1682.
- 14 (a) M. Mahato, G. Rana, P. Kumar and A. K. Sharma, *J. Polym. Sci. Part A: Polym. Chem.*, 2012, **50**, 2344-2355; (b) M. Mahato, P. Kumar and A. K. Sharma, *Mol. BioSyst.*, 2013, **9**, 780-791; (c) M. Mahato, A. K. Sharma and P. Kumar, *Coll. Surf. Biointerfaces*, 2013, **109**, 197-203; (d) M. Mahato, S. Yadav, P. Kumar and A. K. Sharma, *BioMed Res. Int.*, 2014, **2014**, ID 459736.
- 15 D. P. Arya and R. L. Coffee Jr., *Bioorg. Med. Chem. Lett.*, 2000, **10**, 1897-1899.
- 16 M. Chen, J. Wu, L. Zhou, C. Jin, C. Tu, B. Zhu, F. Wu, Q. Zhu, X. Zhu and D. Yan, *Polym. Chem.*, 2011, **2**, 2674-2682.
- 17 M. Chen, M. Hu, D. Wang, G. Wang, X. Zhu, D. Yan and J. Sun, *Bioconjugate Chem.*, 2012, **23**, 1189-1199.
- 18 A. Ghilardi, D. Pezzoli, M. C. Bellucci, C. Malloggi, A. Negri, A. Sganappa, G. Tedeschi, G. Candiani and A. Volonterio, *Bioconjugate Chem.*, 2013, **24**, 1928-1936.
- 19 (a) M. Mahato, V. Arora, R. Pathak, H. K. Gautam, A. K. Sharma, *Mol. BioSyst.*, 2012, **8**, 1742-1749; (b) A. Archut, G. C. Azzellini, V. Balzani, L. D. Cola and F. Vogtle, *J. Am. Chem. Soc.*, 1998, **120**, 12187-12191; (c) S. Patnaik, A. K. Sharma, B. S. Garg, R. P. Gandhi and K. C. Gupta, *Int. J. Pharm.*, 2007, **342**, 184-193.
- 20 C. D. Ciornei, T. Sigurdaróttir, A. Schmidtchen and M. Bodelsson, *Antimicrob. Agents Chemother.*, 2005, **49**, 2845-2850.
- 21 R. Goyal, S. K. Tripathi, S. Tyagi, K. R. Ram, K. M. Ansari, Y. Shukla, D. K. Chowdhuri, P. Kumar and K. C. Gupta, *Eur. J. Pharm. Biopharm.*, 2011, **79**, 3-14.
- 22 R. Kircheis, L. Wightman, A. Schreiber, B. Robitza, V. Rossler, M. Kurska and E. Wagner, *Gene Ther.*, 2001, **8**, 28-40.

- 23 K. A. Gibney, I. Sovadinova, A. I. Lopez, M. Urban, Z. Ridgway, G. A. Caputo, K. Kuroda, *Macromol. Biosci.*, 2012, **12**, 1279–1289.
- 24 Y. Chao and T. Zhang, *Appl. Microbiol. Biotechnol.*, 2011, **92**, 381–392.
- 25 L. Qian, H. Xiao, G. Zhao and B. He, *ACS Appl. Mater. Interfaces*, 2011, **3**, 1895–1901.
- 26 D. M. Copolovici, K. Langel, E. Eriste and U. Langel, *ACS Nano*, 2014, **3**, 1972–1994.
- 27 M. Gupta and V. S. Chauhan, *Biopolymers*, 2011, **95**, 161–173.
- 28 K. Konopka, N. Overlid, A. C. Nagaraj and N. Duzgunes, *Cell. Mol. Biol. Lett.*, 2006, **11**, 171–190.
- 29 (a) U. Lungwitz, M. Breunig, T. Blunk and A. Göpferich, *Eur. J. Pharm. Biopharm.*, 2005, **60**, 247–266; (b) C. Pichon, C. Goncalves, P. Midoux, *Adv. Drug Deliv. Rev.*, 2001, **53**, 75–94.
- 30 M. Ogris, P. Steinlein, M. Kursa, K. Mechtler, R. Kircheis and E. Wagner, *Gene Ther.*, 1998, **5**, 1425–1433.
- 31 P. Kumaraswamy, R. Lakshmanan, S. Sethuraman and U. M. Krishnan, *Soft Matter*, 2011, **7**, 2744–2754.
- 32 M. Chakraborty and A.K. Panda, *Spectrochim. Acta Part A*, 2011, **81**, 458–465.
- 33 O. Pieroni, A. Fissi, R. M. Jain and V. S. Chauhan, *Biopolymers*, 1996, **38**, 97–108.
- 34 (a) K. K. Son, D. H. Patel, D. Tkach and A. Park, *Biochim. Biophys. Acta-Biomembranes*, 2000, **1466**, 11–15; (b) B. Wang, J. Zhou, S. Cui, B. Yang, Y. Zhao, B. Zhao, Y. Duan and S. Zhang, *Afr. J. Biotechnol.*, 2012, **11**, 2763–2773.
- 35 R. F. Epand, M. A. Schmitt, S. H. Gellman and R. M. Epand, *Biochim. Biophys. Acta*, 2006, **1758**, 1343–1350.
- 36 M. D. Seo, H. S. Won, J. H. Kim, T. Mishig-Ochir and B. J. Lee, *Molecules*, 2012, **17**, 12276–12286.
- 37 R. E. W. Hancock, K. L. Brown and N. Mookherjee, *Immunobiol.*, 2006, **211**, 315–322.
- 38 J. Nissen-Meyer and I. F. Nes, *Arch. Microbiol.*, 1997, **167**, 67–77.
- 39 S. Bera, R. Dhondikubeer, B. Findlay, G. G. Zhanel and F. Schweizer, *Molecules*, 2012, **17**, 9129–9141.
- 40 K. Matsuzaki, K. Sugishita, M. Harada, N. Fujii and K. Miyajima, *Biochim. Biophys. Acta*, 1997, **1327**, 119–130.